J Mater Sci (2010) 45:483–489
DOI 10.1007/s10853-009-3965-y

High conductivity and low percolation threshold in polyaniline/graphite nanosheets composites

X. Wu · S. Qi · J. He · G. Duan

Received: 22 July 2009 / Accepted: 5 October 2009 / Published online: 20 October 2009

Abstract An easy process for the synthesis of polyaniline/graphite nanosheets (PANI/NanoG) composites was developed. NanoG were prepared by treating the expanded graphite with sonication in aqueous alcohol solution. Scanning electron microscopy (SEM), X-ray diffraction techniques (XRD), Fourier transform infrared (FT-IR), and transmission electron microscopy (TEM) were used to characterize the structures of NanoG and PANI/NanoG conducting composites. Electrical conductivity measurements indicated that the percolation threshold of PANI/NanoG composites at room temperature was as low as 0.32 vol.% and the conductivity of PANI/NanoG composites was 420 S/cm. The percolation theory, mean-field theory, and excluded volume theory were applied to interpret the conducting properties. Results showed that the low value of percolation threshold may be mainly attributed to nanoscale structure of NanoG forming conducting bridge in PANI matrix and there exists contact resistance in the percolation network formed within PANI/NanoG composites.

Introduction

Due to a great variety of applications in many fields, such as electrochromism, electroluminescence, sensors, and energy storage systems, conducting polymers have become the subjects of increased research interest [1–5]. Although conducting polymers, such as polyaniline (PANI), polythiophene (PTP), polypyrrole (PPy) have been studied extensively in recent years, PANI was one of most studied because of its easy and economic preparation, good environmental stability, and its conductivity that occurs upon doping [6, 7]. However, pure PANI is a non-conducting polymer, in addition, for most doped PANI, the conductivity is typically less than 100 S/cm, and usage of PANI in electronic devices is not yet realistic because charge carriers mobilities are too low to be useful [8]. Graphite, which is naturally abundant and low cost, has been widely used as electronically conducting filler in preparing conducting polymer composites [9, 10].

In order to get a satisfactory conductivity, using conventional graphite powder fillers, polymer composites loadings need about 20 wt% or even higher. However, high graphite powder filler concentration could always lead to not only materials redundancy and detrimental mechanical properties but also a high threshold value (the percolation threshold) [1, 11, 12]. Celzard et al. [13] reported an epoxy/expanded graphite (E.G) composites with a percolation threshold of 1.3 vol.% of E.G fillers by subjecting the graphite powder to a rapid thermal treatment [14]. Recently, several groups reported PMMA/E.G, PS/PG, nylon 6/E.G, PS/PMMA/E.G composites with markedly low threshold values [15–20]. Efimov and coworkers [21] and Meng and coworkers [22] also researched the conductivity of PANI/graphite composites, but the graphite was natural expandable graphite, and the size was at micrometer and millimeter scales. At the basis of these experiments, Chen et al. [23] revealed that the graphite nanosheets (NanoG) were prepared by E.G with ultrasonic irradiation. The NanoG has nanosized (with thickness of 30–80 nm and diameter of 5–20 μm) and the high aspect ratio (diameter to thickness), about 100–300. More recently, NanoG was used to prepare PS/NanoG [24] and PMMA/NanoG [25] composites with very low values of percolation threshold, about 1.6 and 1.5 vol%, respectively.

X. Wu (✉) · S. Qi · J. He · G. Duan
Department of Applied Chemistry, School of Science, Northwestern Polytechnical University, 710129 Xi'an, People's Republic of China
e-mail: Aimar_wu@yahoo.com.cn

In this study, the PANI/NanoG composites were prepared via in situ polymerization of ANI monomer in the NanoG. The morphology and structure were investigated based on scanning electron microscope (SEM), transmission electronic microscopy (TEM), X-ray diffraction techniques (XRD), and Fourier transform infrared (FT-IR). Moreover, the electrical properties of composites in the present case were examined using the percolation theory, mean-field theory, and excluded volume theory.

Experimental details

Materials

Aniline (ANI, chemical pure) from Tianjin Pengfeng chemical company was distilled twice under reduced pressure before use. The conductive filler used here was NanoG prepared by the ultrasonic techniques from E.G [23]. Concentrated hydrogen peroxide, sulfuric acid, 36% hydrochloric acid (HCl), sodium hydroxide (NaOH), and ammonium peroxydisulfate (APS) were used as received.

Synthesis of PANI/NanoG composites

PANI/NanoG composites were prepared using the following procedure. Initially, NanoG powders were oxidized in a solution of NaOH (2 mol/L) at 40 °C for 2 h to improve its surface condition. Secondly, certain amount of surface-treated NanoG, ANI, 36% hydrochloric acid, and redistilled water were placed in an ultrasonic bath and treated for 30 min at room temperature. Then the APS at appropriate concentration was added to the reaction media in a dropwise fashion for 1 h using a dropping funnel. The polymerization temperature was kept 0–5 °C and the reaction time was 8 h after APS of aqueous solution was added wholly. Upon being filtered, the precipitates were washed with redistilled water and ethanol repeatedly. The solids were dried under vacuum at ambient temperature for 24 h. A schematic illustration of the fabrication process of PANI/NanoG composites is shown in Fig. 1.

Measuring methods

Dry powdered samples were made into pellets using a steel die of 2.0 cm diameter in a hydraulic press under a pressure of 20 MPa. The conductivities of the PNAI/NanoG composite samples were measured at room temperature using SZ-82 digital four probes resistance tester (Suzhou Electronic Equipment Company) and the conductivity values were calculated directly from the measured resistance and sample dimensions. Fourier transform infrared (FT-IR) of the samples in KBr pellets were recorded on a WQF-31 model FT-IR spectrometer (China). X-ray diffraction patterns were recorded for the structural characterization of NanoG and PANI/NanoG composites on powder samples by a X'Pert MPDPRO instrument (PANalytical, Holland). Scanning electron microscope (SEM; JSM-6360LV JEOL Company, Japan) was used to observe the morphologies of NanoG and PANI/NanoG composite. Transmission electron microscopy (TEM) was performed with the H-800 model transmission electron microscope (HITACHI Company, Japan) at 100 kV accelerated voltage. The massive composites were then microtomed with an IB-V ultrotometer apparatus into slices. Subsequently, the observations were carried out after retrieving the slices onto Cu grids.

Results and discussion

Microstructures of NanoG and PANI/NanoG composites

We sonicated the expanded graphite in alcohol solution using ultrasonic irradiation technique and then obtained NanoG. Figure 2a, b shows the SEM micrograph of the as-prepared NanoG. It reveals that the NanoG are obtained with thickness about 30 nm and a diameter of 1–20 μm. The prepared NanoG possessed a high aspect ratio (width-to-thickness) of around 100–500. It demonstrates that the NanoG are very thin and endowed with the large surface area, which is one excellent property that was responsible for the formation of a high electrical conductivity within the PANI or coating material at very low values of percolation threshold. This has also been seen in the PANI/NanoG composites of SEM and TEM micrograph shown in the following part. The result is similar to that reported by other researchers [23, 26–28].

The typical SEM pictures of PANI/NanoG composites presented in Fig. 3a and b are SEM micrographs of fracture surface and surface, respectively. The composites show a uniform distribution of small particles in NanoG and PANI

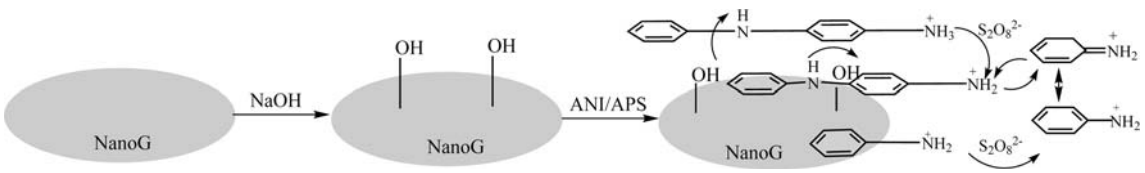

Fig. 1 Pictorial representation of the synthesis of PANI (oxidative polymerization process of aniline by APS) on a graphite nanosheet surface

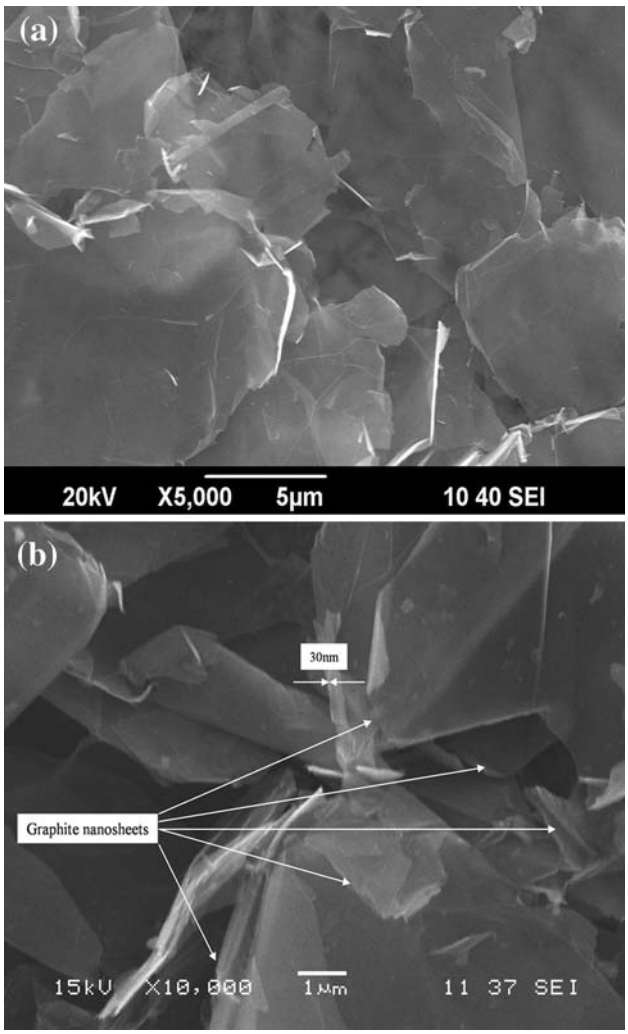

Fig. 2 SEM micrograph of graphite nanosheets **a** 5.0×10^3 magnification and **b** 1.0×10^4 magnification

matrix; the NanoG dispersed in PANI matrix and the PANI also embedded in the NanoG are clearly observed. Furthermore, NanoG is distributed quite uniformly within the PANI matrix. Due to this especial structure, we estimate that conduction property of PANI/NanoG composites may be controlled by the NanoG's special structure and reveal a low value of percolation threshold; this result was researched in the following part.

Figure 4 shows X-ray diffraction patterns of PANI and PANI/NanoG composites, respectively. As shown in Fig. 4b, the PANI/NanoG composites showed unusual crystallinity. A sharp peak located at $2\theta = 30.8°$ is a typical diffraction peak of graphite. For pure PANI, however, the peak's intensity was almost the same as that of PANI/NanoG composites besides the graphite diffraction peak because we use same method to prefabricate PANI. This result suggested that the existence of NanoG made no difference to the PANI crystallinity and therefore affect the conductivity of the composites.

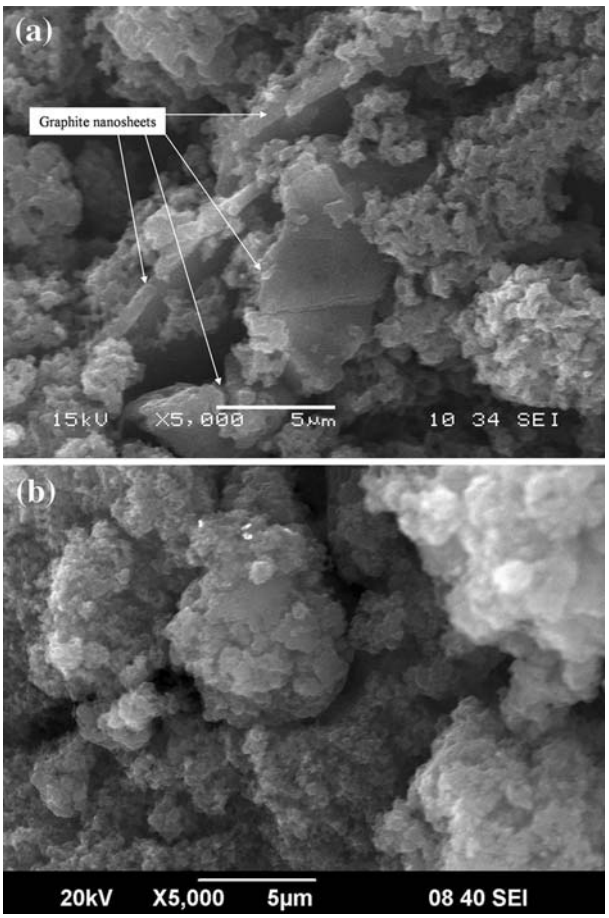

Fig. 3 SEM micrograph of PANI/NanoG composites **a** fracture surface and **b** surface

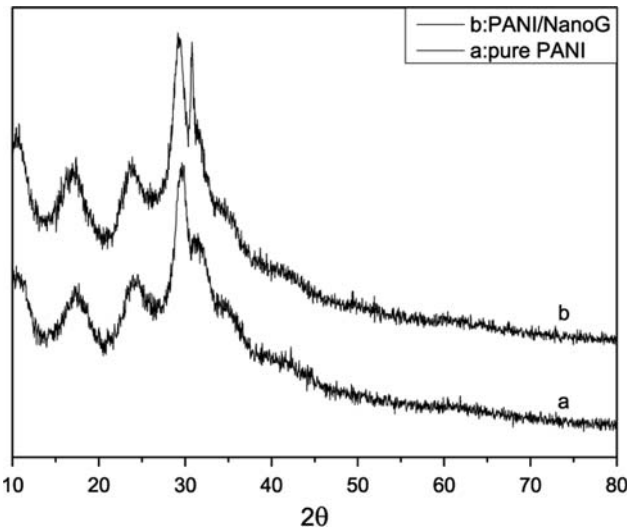

Fig. 4 X-ray diffraction patterns of pure PANI and PANI/NanoG composites

The FT-IR spectra of the prepared pure PANI (Fig. 5) clearly exhibited characteristic absorption peaks with respect to pure PANI. The absorption at 794 cm^{-1} was

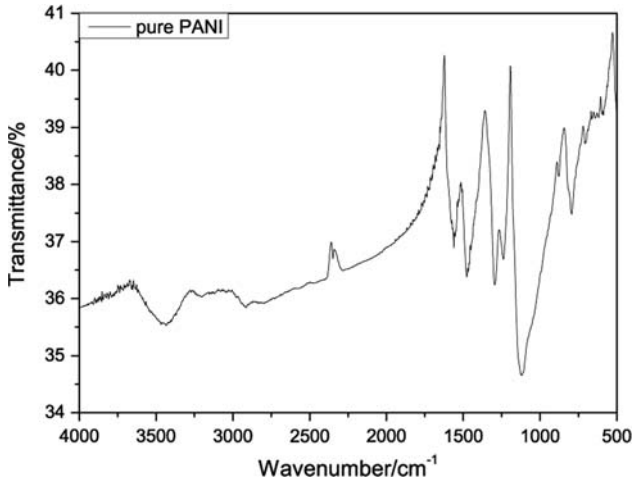

Fig. 5 FT-IR absorption spectra of pure PANI

related to the C–H outerbending vibration. The broad band from 1000 to 1400 cm^{-1} was attributed to C–N or C–H in-plane deformation modes and had a maximum at 1119 cm^{-1}. The band at 3435 cm^{-1} corresponded to the N–H stretching vibration and that at 1477 cm^{-1}, 1560 cm^{-1} reflected C=C stretching vibration. The above results indicated the formation of PANI. From Fig. 6 remarkable differences between PANI/NanoG composites and pure PANI could be observed. The N–H stretching vibration at 3435 cm^{-1} was obvious in the pure PANI, yet not clear in the PANI/NanoG composites. Meanwhile, the characteristic peaks of the PANI molecules in the composites shifted to lower wavenumbers. This may be reasonably concluded that there was strong interaction between PANI and NanoG. The addition of NanoG surface resulted in the formation of hydrogen bonding (it can be explain in Fig. 1), which weakened the N–H as well as its stretching intensity. The evidences indicated that the

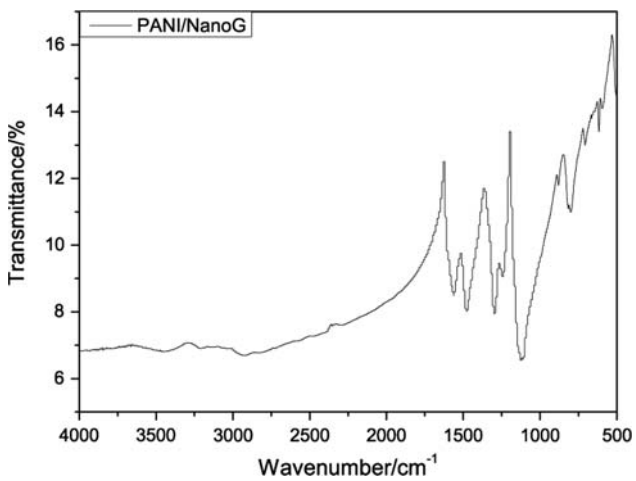

Fig. 6 FT-IR absorption spectra of PANI/NanoG composites

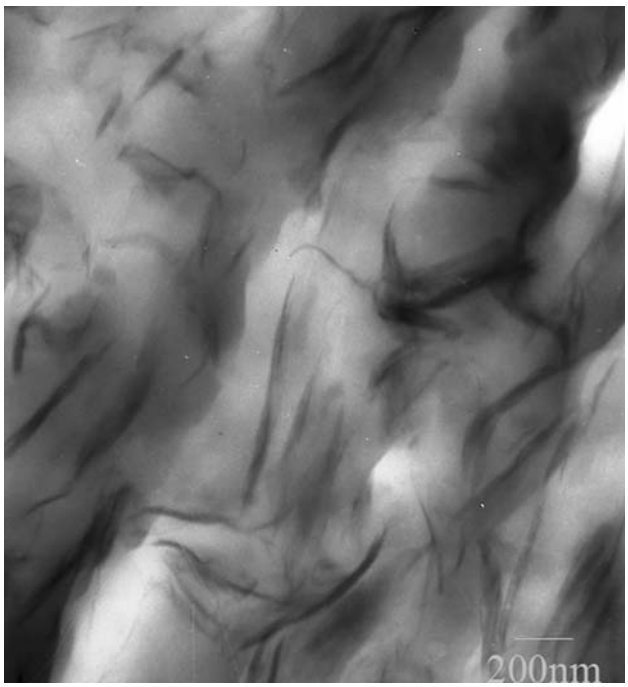

Fig. 7 TEM micrograph of PANI/NanoG composites

PANI/NanoG composites were successfully synthesized by in situ polymerization of aniline monomer and NanoG.

Figure 7 shows TEM images of PANI/NanoG composite slice. The dark lines are the graphite nanosheets, and the dark spot represented the in the cross section of PANI/NanoG nanocomposite. It is apparent that the thickness of NanoG ranged from 30 to 100 nm and the NanoG are randomly dispersed in the PANI matrix forming effective conductive network. The conductive network is believed to lead to the greatly improved electrical conductivity for the composite. The more extreme the geometry of the NanoG was, the lower the conductive filler load and excellent composite's conductive property was, and subsequently lower was the percolation threshold.

Electrical conducting properties and theoretical interpretation

Percolation theory

Variations of electrical conductivities of the PANI/NanoG with respect to filler content are displayed in Fig. 8. As the NanoG increases, the electrical conductivity of PANI/NanoG increases gradually as well. It reaches 522 S/cm at 4.5 vol.%, which is about one hundred times than that of pure doped PANI (5 S/cm). A feature in this figure is that in the PANI/NanoG composites an abrupt conductivity transition occurs at critical filler content, which can be designated as the percolation threshold. So we can infer

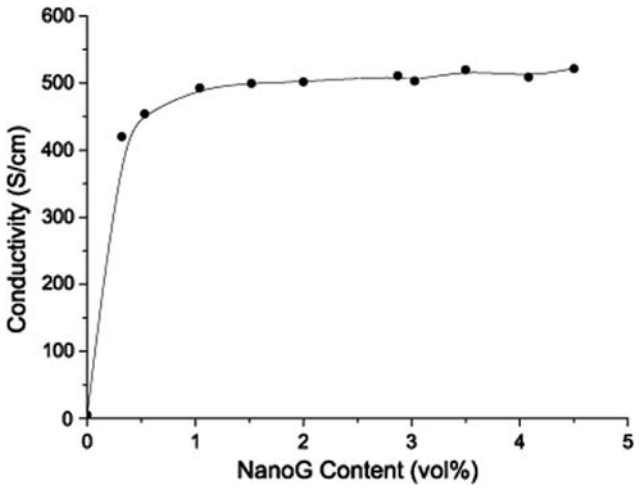

Fig. 8 Electrical conductivity of PANI/NanoG as a function of the NanoG contents

that the percolation threshold of PANI/NanoG composites is about 0.32 vol.%; the advantage of NanoG as a conductive polymer in PANI is significant.

According to classical percolation [29], the dependence of the electrical conductivity of PANI/NanoG composites on the NanoG content can be described in Eq. 1, where σ_m is the PANI/NanoG composites conductivity, σ_n is the conductivity of NanoG, v is the volume fraction of NanoG, v_c is the percolation threshold, β is the critical exponent which is 2 and 1.3 for three-dimensional and two-dimensions randomly distributed nanocomposites, respectively, in the percolation model. The experimental data presented in Fig. 8 for PANI/NanoG thus are fitted using Eq. 1 and the results are plotted in Fig. 9. As shown in Fig. 9, the critical exponent for PANI/NanoG is $\beta = 0.85$ which is lower than the universal one. This suggests that the pure doped PANI electrical conductivity is about 5 S/cm which is much higher

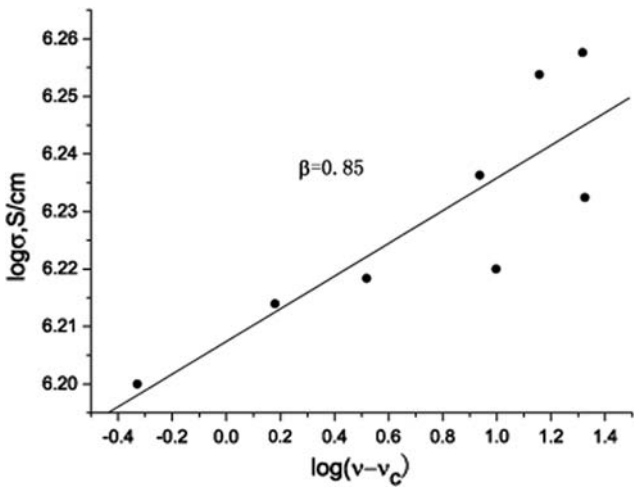

Fig. 9 Fits of the conductivity data in Fig. 8 using Eq. 1

than conventional non-conductive polymer (about 10^{-12} S/cm) and the NanoG has a large aspect ratio (about 100–500) which can be observed in the SEM photograph of NanoG and in the TEM photograph of PANI/NanoG. Such an extreme geometry might be a factor contributable to the high electrical conductivity and low critical exponent.

The result is the low value of the percolation threshold v_c, 0.32% much lower than that of composites with conventional graphite filler (about 2–5 vol.%) [24]. Hence, it is evident that the NanoG with extreme geometry (high aspect ratio) is more effective in forming conducting network and bring about lower percolation threshold. In the following sections, theoretical interpretations of low percolation threshold will be discussed according to the Mean-field theory.

$$\sigma_m = \sigma_n (v - v_c)^{\beta} \tag{1}$$

Mean-field theory

Helsing and Helte [30] and Lu et al. [14] reported an approach to calculate the percolation threshold. Its theory is based on calculating the average effect of the random resistor network by approximating the mixture of polymer and conductive filler as a homogeneous effective system. Consequently, the empirical formula has been given

$$v_c = 1.18\eta \tag{2}$$

where η is the ratio of major axis length γ_1 and minor axis length γ_2.

In our case, the average diameter of NanoG is 10 μm and the average thickness is 30 nm, so the NanoG can be approximately described as this type of subject with η (30 nm/10 μm) of 0.003, the percolation threshold for PANI/NanoG composites will be

$$v_c = 0.354\% \tag{3}$$

Obviously, this result is about the same comparable to the value 0.32% in our case. Similarly, Ruschau and Newnham [31] regarded that a conductive polymer composites were a conductive backbone with a certain packing density, which was different from the conducting powder according to the conductive filler morphologies. As far as conductive filler of traditional polymer composites are concerned, the percolation threshold is between 20 and 50%. According to this theory, the relation between the percolation threshold v_c and the conductive filling factor v_p can be described by a simple power law:

$$v_c = v_p \pm 5\% \tag{4}$$

where v_p is the density of material constituting this conductive filler. Lu et al. [14] found that if the percolation threshold is below 20%, the v_c and v_p are approximately equal ($v_c \approx v_p$). Now, we apply this equation to calculate the percolation threshold of PANI/NanoG composites.

In our case, although the accurate density of material constituting this NanoG is not easy to obtain, we know that the apparent density of the NanoG is about 0.015 g/cm^3 and the mass density of PANI/NanoG composites is 4.41 g/cm^3.

So the percolation threshold $v_c \approx v_p$ (0.015/4.41) of about 0.34% could then be obtained. This value is also close to fit the value of experiment.

In conclusion, mean-field theory indicates that high aspect ratio of the NanoG leads to a lower percolation threshold. In order to further verify the correctness of experimental result, we will further interpret according to the excluded volume theory.

Excluded volume theory

From the above we know that using the NanoG with high aspect ratio can achieve high conductivity and low percolation threshold in preparing PANI/NanoG composites. Balberg et al. [32] proposed the concept of excluded volume, the volume around an object to the center of another similar object is not allowed to enter if overlapping of the two objects is to be avoided.

Based on the above assumptions, in our case, the excluded volumes of the NanoG are able to overlap and form conducting network in PANI matrix, which can be observed in the TEM photograph of PANI/NanoG composites. Therefore, the percolation threshold is related to excluded volume of the NanoG rather than the real volume of PANI/NanoG composites. Now, we define the total excluded volume in the form as follows.

$$(E_{\mathrm{VX}}) = N_e(E_{\mathrm{V}}) \tag{5}$$

where (E_{VX}) is the excluded volume of conductive filler averaged over the oriental distribution characterizing the composites, N_e is the critical number density of conductive filler in the composites, and E_{V} is the associated volume. In fact, (E_{VX}) is a variable and situated for each object within a range of values corresponding to the system characterized by a random orientation (low limit) and a system of strictly parallel conductive fillers or objects (upper limit). The critical volume concentration in three dimensions is linked to (E_{VX}) by [14, 31, 32]

$$v_c = 1 - \mathrm{e}^{-(E_{\mathrm{VX}})V/E_{\mathrm{V}}} = 1 - \mathrm{e}^{-N_e V} \tag{6}$$

where E is the volume of a pore.

Because the NanoG is about disk-shaped, the percolation threshold can be related to the thickness and radius of the NanoG by

$$v_c = 1 - \mathrm{e}^{-(V_{\mathrm{EX}})d/\pi r} \tag{7}$$

where r is the radius and d is the thickness of the NanoG. Because the value of (E_{VX}) is expected to lie between 1.8 and 3.8, the expression of v_c for [33] is

$$1 - \mathrm{e}^{-1.8d/\pi r} \le v_c \le 1 - \mathrm{e}^{-3.8d/\pi r} \tag{8}$$

In this case, the thickness of NanoG is 30 nm and the radius is 10 μm, the critical volume fraction of PANI/NanoG composites is found to be:

$$0.17 \le v_c \le 0.36\% \tag{9}$$

The value of v_c, 0.32%, falls within this range. This result amply confirms that high aspect ratio of the NanoG leads to a lower percolation threshold.

Conclusions and outlook

In this paper, PANI/NanoG composites and its electrical properties have been investigated. SEM micrograph reveals that the NanoG are with thickness about 30 nm and a diameter of 1–20 μm. The dispersion of NanoG within the PANI have evidenced by SEM, TEM, XRD, and FT-IR examinations. Electrical conductivity measurements have indicated that the percolation threshold of PANI/NanoG composites at room temperature was as low as 0.32 vol.% and the conductivity of PANI/NanoG composites was 420 S/cm. To interpret this low fitted value caused by high aspect ratio of NanoG in the PANI, mean-field theory and excluded volume theory are applied, and we found out that the special morphology of NanoG plays an important role in minimizing the percolation threshold. Because the application range of PANI/NanoG composites is limited owing to their conductivity, to improve the conductivity of composites further, we chose silver for coating NanoG surface, and then synthesize by in situ polymerization with aniline monomer. Additional research on multi-functional PANI composites is required. For example, nickel plating NanoG as filler in PANI matrix fabricate PANI composites will enormously enhance electromagnetism performance of PANI. In the future, our team will research the preparation methods and performance of the new PANI composites.

Acknowledgements The authors appreciate the help of Ms. Shi for SEM photograph and thank Ms. Li Liefeng for the TEM photograph. The authors are also thankful to the companies and relatives who kindly offered the materials and help.

References

1. Pinto G, Jimenez-Martin A (2001) Polym Compos 22:65
2. Hepel M (1998) J Electrochem Soc 145:124
3. Flandin L, Bidan G, Brechet Y, Cavaile JY (2000) Polym Compos 21:165
4. Wessling B, Posdorfer J (1999) Electrochim Acta 44:2053
5. Roldughin VI, Vysotskii VV (2000) Prog Org Coat 39:81
6. Sapurina I, Mokeev M, Lavrentev V (2000) Eur Polym J 36:2321
7. Wang DH, Qi SH, Wu YM (2009) J Appl Polym Sci 110:3162
8. Xiao P, Xiao M, Liu PG, Gong KC (2000) Carbon 38:623

9. Shioyama H, Tatsumi K, Iwashita N (1998) Synth Met 96:229
10. Xiao M, Sun L, Liu J (2002) Polymer 43:2245
11. Kirkpatrick S (1973) Rev Mod Phys 45:574
12. Carmona F (1989) Physica A 157:461
13. Celzard A, Mareche JF, Furdin G (2000) Phys D Appl Phys 33:3094
14. Lu W, Lin HF, Wu DJ (2006) Polymer 47:4440
15. Chen GH, Wu DJ, Weng WG (2001) Polym Int 50:980
16. Wenge Z, Shing CW (2002) Polymer 73:6767
17. Chen GH, Wu DJ, Weng WG (2001) Acta Polym Sin 6:803
18. Xiao P, Xiao M, Gong K (2001) Polymer 42:4813
19. Chen GH, Wu DJ, Weng WG (2001) J Appl Polym Sci 82:2506
20. Pan YX, Yu ZZ, Ou YC (2000) J Polym Sci Part B Polym Phys 38:1626
21. Tchmutin IA, Ponomarenko AT, Efimov ON (2003) Carbon 41:1391
22. Du XS, Xiao M, Meng YZ (2004) Eur Polym J 40:1489
23. Chen GH, Weng WG, Wu DJ (2004) Carbon 42:753
24. Chen GH, Weng WG, Wu DJ (2003) Eur Polym J 39:2329
25. Chen GH, Wu DJ, Weng WG (2003) Polymer 44:1781
26. Habsuda J, Simon GP, Cheng YB (2002) Polymer 44:4627
27. Wang JJ, Zhu MY, Outlaw-Ron A (2004) Carbon 42:2867
28. Mo ZL, Zuo DD, Chen H (2007) Eur Polym J 43:300
29. Stauffer D, Aharony A (1991) Introduction to percolation theory. Taylor & Francis, London
30. Helsing J, Helte A (1991) J Appl Phys 69:3583
31. Ruschau GR, Newnham RE (1992) J Compos Mater 26:2727
32. Balberg I, Anderson CH, Alexander S (1984) Phys Rev B 30:3933
33. Hu YH, Liu JF, Dong HB (1998) Polym Sci Eng 14:59